Pedosphere **36**(2): 497–510, 2026
doi: 10.1016/j.pedsph.2024.11.002
ISSN 1002-0160/CN 32-1315/P

Published by Elsevier B.V. and Science Press

PEDOSPHERE

www.elsevier.com/locate/pedosphere

Artificial humic acid promotes carbon sequestration in the rice-soil system

Zeyu ZHANG[1,2], Yu QIAO[1,2], Dongxing XIE[1,2], Jicheng HAN[1,2], Zhuqing LIU[1,2], Ying ZHAO[1,2,*] and Fan YANG[1,2,*]

[1]*International Cooperation Joint Laboratory of Health in Cold Region Black Soil Habitat of the Ministry of Education, Harbin 150030 (China)*
[2]*School of Water Conservancy & Civil Engineering, Northeast Agricultural University, Harbin 150030 (China)*

(Received June 17, 2024; revised August 20, 2024; accepted October 29, 2024)

ABSTRACT

Artificial humic acid (AHA) is a new exogenous organic material with enormous carbon (C) sequestration potential. However, the effects of applying AHA under different irrigation regimes on C sequestration in the rice-soil system and the underlying mechanisms still need to be clarified. This study employed C isotope labeling technology to analyze the photosynthetic C sequestration capacity, C transport capacity of rice roots, and greenhouse gas emission flux in the rice-soil system under different irrigation regimes and AHA application conditions. The results showed that as the amount of AHA application increased, the leaf area and chlorophyll concentration gradually increased, and the ribulose-1,5-bisphosphate carboxylase/oxygenase (Rubisco) activity first increased and then decreased under two irrigation regimes (conventional flooding and alternate wetting and drying irrigation). In the alternate wetting and drying irrigation with 300 mg kg^{-1} AHA application treatment (DWI3), the photosynthetic C fixation was the highest, with the net photosynthetic rate increasing by 65.35% compared to the alternate wetting and drying irrigation without applying AHA treatment (DWI0). Meanwhile, the organic acid concentration in root exudates, biomass, length, surface area, and length density were also the highest in the DWI3 treatment. Besides, the content of ^{13}C in soil was the highest in the DWI3 treatment, closely related to the strongest photosynthetic C fixation and root transport capacity, as well as the lowest greenhouse gas emission flux. Therefore, it is recommended to apply 300 mg kg^{-1} AHA with alternate wetting and drying irrigation for C sequestration, water conservation, and sustainable agricultural development.

Key Words: alternate wetting and drying irrigation, C isotope labeling, chlorophyll fluorescence, conventional flooding irrigation, isotope tracing technology, photosynthesis, root exudates

Citation: Zhang Z Y, Qiao Y, Xie D X, Han J C, Liu Z Q, Zhao Y, Yang F. 2026. Artificial humic acid promotes carbon sequestration in the rice-soil system. *Pedosphere*. **36**(2): 497–510.

INTRODUCTION

Covering approximately 165 million ha worldwide, paddy soils have enormous carbon (C) sequestration potential (Chen *et al*., 2021). At the same time, the long-term flooding environment in paddy fields also causes significant loss of water resources. According to statistics, the irrigation water in paddy fields is about 2.5 times that of other crops such as corn and wheat (MWR, 2020). In recent years, alternate wetting and drying irrigation has received widespread attention due to its advantages of water conservation and improvement of soil redox conditions (Dodd *et al*., 2015; Runkle *et al*., 2019). In the paddy field ecosystem, water management is a crucial factor affecting crop growth and soil C cycling (Alavaisha *et al*., 2022). Long-term flooding may lead to deterioration of soil structure, decrease soil permeability and aeration, and affect root growth and soil C sequestration capacity (Martínez-Alcántara *et al*., 2012). Although alternate wetting and drying irrigation can improve water use efficiency, it may limit rice plant growth and affect photosynthesis and C sequestration (Carrijo *et al*., 2017). Especially during the dry stage, alternate wetting and drying irrigation may cause fluctuations in soil C emissions, accelerate the mineralization rate of soil organic matter, and lead to a short-term increase in C emissions (Liao *et al*., 2020). Therefore, a large number of scholars try to alleviate these problems by applying exogenous organic materials (Grunwald *et al*., 2018; Tian *et al*., 2019; Wang *et al*., 2020). Artificial humus acid (AHA) is a new type of exogenous organic material with a highly similar composition and function to natural humus but a considerably shortened production time. It utilizes waste biomass rich in lignin as raw material and generates humus-like substances with significant C fixation and fertilization effects through a new hydrothermal humification reaction (Yang *et al*., 2019; Zhao *et al*., 2024). Previous studies have shown that it can improve soil structure, promote aggregate formation, increase organic matter content, and enhance nutrient availability in soil (Tang *et al*., 2022). However, the effects and mechanisms of AHA application on soil C sequestration under conventional flooding and alternate wetting and drying irrigation are still unclear.

*Corresponding author. E-mail: yangfan_neau@163.com, zhaoying@neau.edu.cn.

Soil C sequestration is influenced by C cycling processes in the plant-soil system, including plant photosynthetic C sequestration, root transport, and greenhouse gas emissions (Jansson *et al*., 2010; Whalen *et al*., 2014; Harman *et al*., 2021; Sasse, 2023). First, plants fix atmospheric CO_2 in their leaves through photosynthesis (Gayathri *et al*., 2021). Photosynthesis is a complex physiological process with numerous influencing factors, among which photosynthetic pigment concentration and ribulose-1,5-bisphosphate carboxylase/oxygenase (Rubisco) activity are two key factors (Gujjar *et al*., 2020; Sidhu *et al*., 2021). Chlorophyll is a critical pigment that captures light energy in photosynthesis, and its content directly affects the efficiency of light energy capture in photosynthesis (Wu *et al*., 2019). Carotenoids (Carots) protect chloroplasts from damage by quenching excess excited-state energy (Young, 1991). Rubisco plays a vital role in photosynthesis and photorespiration. Higher plants and green algae optimize CO_2 fixation and substrate regeneration by regulating Rubisco activity, ensuring optimal photosynthesis under various environmental conditions (Salvucci, 1989). Second, some photosynthetic products fixed in leaves are actively transported to roots through the phloem and metabolized in roots (Ainsworth and Bush, 2011). Plants produce root exudates through root metabolism activities, and their organic acids can affect soil C sequestration through various pathways (Lei *et al*., 2023). Approximately 5%–21% of photosynthetic C is transferred underground through root exudates (Tang *et al*., 2021). Complex interactions between root exudates, root aeration tissue, and root activity affect plant growth, health, and environmental adaptability (Vives-Peris *et al*., 2020; Huang *et al*., 2021). In addition to root exudates, root biomass and root morphology characteristics are also important indicators for evaluating root C transport capacity (Wang J S *et al*., 2021; De Pessemier *et al*., 2022). Finally, some organic C fixed in soil will be released into the atmosphere through greenhouse gases such as CO_2 and CH_4(van Groenigen *et al*., 2011). Overall, soil C sequestration is a dynamic process that involves the fixation of CO_2 in the atmosphere through photosynthesis, the transport of organic C from roots to soil, and the interaction between soil and plant respiration in the plant-soil system. These processes collectively determine the accumulation and loss of organic C in soil, affecting the soil ability of acting as a C sink. Effective soil C sequestration management requires comprehensive consideration of these processes to maximize soil C storage potential and reduce greenhouse gas emissions. However, the effects of different irrigation regimes, when combined with the application of AHA, on the processes of photosynthetic C sequestration and C transport in the rice-soil system remain unclear.

Isotope tracing technology is essential for quantifying C allocation and studying C transport dynamics (Kuzyakov and Schneckenberger, 2004). Significant progresses have been made in tracking the sources of soil organic C (SOC), evaluating the relative contributions of new and old SOC, and the influencing factors of soil respiration using isotope techniques, namely ^{13}C or ^{14}C continuous or pulse labeling (Liu *et al*., 2019; Wang R Z *et al*., 2021). Therefore, this study used ^{13}C isotope tracing technology to trace the dynamics of photosynthetic C in the rice-soil system and assess the effects of AHA application on the sequestration and transport of photosynthetic C in rice plants under flooding and alternate wetting and drying irrigation. This study aimed to: i) quantify the input and allocation of photosynthetic C in the rice-soil system, ii) identify the fundamental mechanisms that affect soil C sequestration, and iii) evaluate the most suitable irrigation and AHA application scheme for soil C sequestration.

MATERIALS AND METHODS

Preparation of AHA

The AHA used in this study was prepared using the hydrothermal humification method from our previous study (Du *et al*., 2020). Rice straw powder (24 g) sieved through a 0.15-mm mesh was amended with KOH particles (6 g) and ultra-pure water (220 mL), reacting in a reaction vessel at 200 °C for 24 h. After reaction, the mixture was cooled with water and filtered, and the pH of the liquid AHA was adjusted to 1 with 2.0 mol L^{-1} HCl to obtain solid AHA. The AHA solid was centrifuged with ultra-pure water to neutrality, followed by drying in an oven at 80 °C. The C, nitrogen (N), sulfur, and hydrogen (H) contents in AHA were 637.3, 12.1, 6.3, and 58.5 g kg^{-1}, respectively. The scanning electron microscopy images of AHA used in this study are shown in Fig. 1.

Experimental design

The experimental soil was loamy, taken from the 0–20 cm topsoil layer near Northeast Agricultural University, China. After natural air drying, the soil was sieved through a 2-mm sieve, with 7 kg soil per pot. Selected soil physical and chemical properties are shown in Table I. Twenty-five-day-old seedlings of the rice variety Longjing 24 were transplanted into PVC pots (12 cm in inner diameter, 50 cm in height), with three plants per pot. The experiment was conducted in a climate chamber from May 20 to July 7, 2023, with day/night temperature of 30 ± 1 °C/25 ± 1 °C, relative humidity of 80%–90%, a light cycle of 12 h (from 8:00 a.m. to 8:00 p.m. every day), and a light intensity of 500 μmol photons m^2 s^{-1}. The rice plants were watered with deionized water during rice growth and timely weeded. Basal fertilizers were applied before rice planting at 40 mg N kg^{-1} soil, 20 mg phosphorus kg^{-1} soil, and 80 mg potassium kg^{-1} soil, respectively.

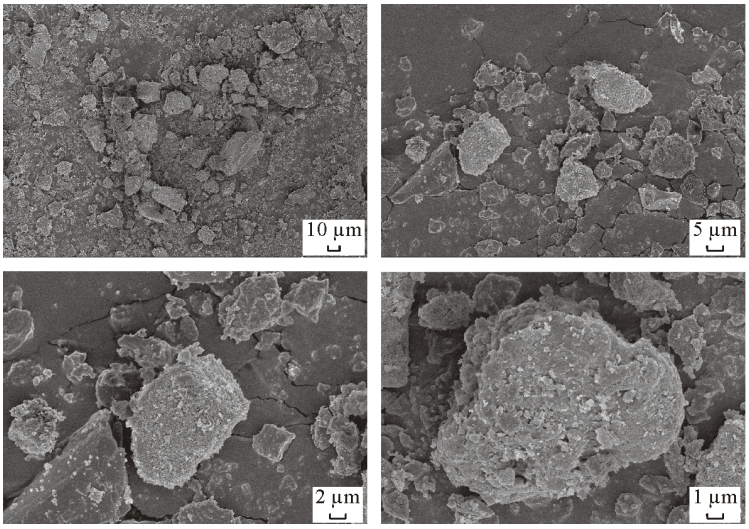

Fig. 1 Scanning electron microscopy images of the artificial humic acid used in this study.

TABLE I

Selected physical and chemical properties of the soil used in this study

Property	Unit	Value
Bulk density	g cm^{-3}	1.4
pH		6.9
Field capacity	cm^3 cm^{-3}	24
SOC[a)] content	g kg^{-1}	21
Total N	g kg^{-1}	1.05
Total P	g kg^{-1}	0.32

[a)] Soil organic C.

TABLE II

Experimental design of this study

Treatment code	Irrigation regime[a)]	AHA[b)] application amount
		mg kg^{-1} soil
GI0	GI	0
GI3	GI	300
GI6	GI	600
DWI0	DWI	0
DWI3	DWI	300
DWI6	DWI	600

[a)] GI = conventional flooding irrigation; DWI = alternate wetting and drying irrigation.
[b)] Artificial humic acid.

The experimental setup included the irrigation regime (conventional flooding and alternate wetting and drying irrigation) and the amount of AHA application (0, 300, and 600 mg kg^{-1} soil). The conventional flooding irrigation treatment maintained a water surface height of 2–3 cm in a PVC pot. The alternate wetting and drying irrigation maintained a 2–3 cm water layer within 7 d after transplanting to ensure the greening and survival of rice, with alternate wetting and drying irrigation for the rest of the time. Upon natural drying of the surface and attainment of a soil water potential of −15 kPa, a 2–3 cm water layer was applied through irrigation. There were a total of six treatments, including conventional flooding irrigation with AHA at 0 (GI0), 300 (GI3), and 600 (GI6) mg kg^{-1} soil and alternate wetting and drying irrigation with AHA at 0 (DWI0), 300 (DWI3), and 600 (DWI6) mg kg^{-1} soil, each with six replicates (Table II).

$^{13}CO_2$ pulse labeling. Isotope labeling was conducted based on Ge *et al*. (2012) and Liu *et al*. (2023). After 25 d in a PVC pot, the rice plants of three replicates of each treatment were moved into a labeling chamber (100 cm × 50 cm × 85 cm, 5-mm thick) (Fig. 2). Before isotope labeling, the labeling chamber was inserted into the base groove, and the groove was sealed with water. A real-time CO_2 monitor with temperature, humidity, and CO_2 probes was used in the labeling chamber to record internal temperature, humidity, and CO_2 concentration. A rechargeable electric fan was used to promote gas mixing. Using 99 atom% $^{13}CO_2$ pulse labeling, $^{13}CO_2$ concentration was maintained at 350 μL L^{-1}. The marked time was from 7:00 a.m. to 6:00 p.m. on June 15 to 17, 2023. At the same time, the non-pulsed rice plants, those of the remaining three replicates of each experiment, were cultivated 10 m away from the labeled chamber as a natural abundance control of $^{13}CO_2$.

Sampling

Destructive sampling was conducted for each treatment, selecting three pots of labeled and unlabeled rice plants, respectively, on the 20th day after $^{13}CO_2$ labeling. Firstly, shoots were cut off, roots were separated from soil and rinsed clean with deionized water, and then the shoots and roots were dried at 105 °C for 30 min and at 60 °C to a constant weight. The plant samples were crushed into powder. The soil samples were collected, dried naturally, and sieved through a 0.15-mm sieve for further determination of the abundance of ^{13}C.

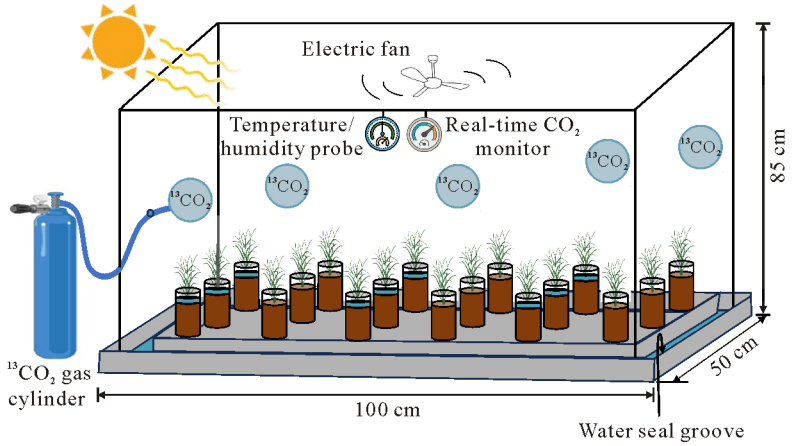

Fig. 2 Diagram of the isotope labeling device used in this study. Chambers with and without blue layers indicate treatments under conventional flooding irrigation and alternate wetting and drying irrigation with artificial humid acid at 0, 300, and 600 mg kg^{-1} soil, respectively.

^{13}C abundance and allocation ratio calculation

The ^{13}C abundance ($At^{13}C\%$, ‰) in plant leaves, stems, and roots, as well as soil, was determined as follows:

$$At^{13}C\% = \left(\frac{R_{sample}}{R_{V\text{-}PDB}} - 1\right) \times 1\,000 \quad (1)$$

$$^{13}C_s = C_{sample} \times (At^{13}C_l - At^{13}C_{nl}) \quad (2)$$

where R_{sample} and $R_{V\text{-}PDB}$ are the $^{13}C/^{12}C$ ratios of the sample and the standard substance (Vienna-Pee Dee Belemnite (V-PDB), 0.0112372), respectively, $^{13}C_s$ (mg kg^{-1}) is the ^{13}C content in the sample, C_{sample} (mg kg^{-1}) is the total C content in the sample, and $At^{13}C_l$ and $At^{13}C_{nl}$ are the $At^{13}C$ in the labeled and unlabeled samples, respectively.

The distribution proportion of assimilated ^{13}C ($^{13}C_p$, %) in various parts of rice plants (leaves, stems, or roots) or soil was calculated as follows:

$$^{13}C_p = \frac{^{13}C_x}{^{13}C_{leaf} + {}^{13}C_{stem} + {}^{13}C_{root} + {}^{13}C_{soil}} \quad (3)$$

where $^{13}C_{leaf}$, $^{13}C_{stem}$, $^{13}C_{root}$, and $^{13}C_{soil}$ (%) are the distribution proportions of assimilated ^{13}C in leaves, stems, roots, and soil, respectively, and $^{13}C_x$ represents the $^{13}C_{leaf}$, $^{13}C_{stem}$, $^{13}C_{root}$, or $^{13}C_{soil}$.

Measurement of rice leaves

Gas exchange parameters, including the net photosynthetic rate (P_n), intercellular CO_2 concentration (C_i), stomatal conductance (G_s), and transpiration rate (T_r), of rice flag leaves were measured using a portable photosynthesis system (LI-6400, Li-COR, USA) every 5 d within 20 d after C isotope labeling. During the measurement period, the leaf temperature was maintained at 28 ± 1.0 °C, the photosynthetic photon flux density was 1 500 μmol m^{-2} s^{-1}, and the CO_2 concentration was maintained at 400 μmol mol^{-1}, with a relative humidity of 40%. Data were recorded after reaching a steady state (about 15 min).

On the same day of measuring gas exchange parameters, three rice plants were randomly selected for each treatment for the following measurements. Chlorophyll concentration was measured on the mid-section of the flag leaves (avoiding the major veins) using 80% acetone. The absorbance of each pigment was measured using a UV spectrophotometer (UV2550, Shimadzu Co., Ltd., Japan). Chlorophyll *a* (Chl*a*) and *b* (Chl*b*) and Carot concentrations were calculated using the Beer-Lambert formula as follows:

$$Chla = 12.21 \times A_{663} - 2.81 \times A_{646} \quad (4)$$

$$Chlb = 20.13 \times A_{646} - 5.03 \times A_{663} \quad (5)$$

$$Carot = \frac{1\,000 \times A_{470} - 3.27 \times Chla - 104 \times Chlb}{229} \quad (6)$$

where A_{663}, A_{646}, and A_{470} are the absorbance of chloroplast pigment extract at wavelengths of 663, 646, and 470 nm, respectively.

The leaf tissue was homogenized with the extraction buffer at 0–4 °C, and the Rubisco solution was obtained by centrifugation. Rubisco activity was measured using Microplate Reader (Infinite 200Pro, Tecan AG, Switzerland) at a wavelength of 450 nm.

Leaf area was measured using a portable leaf area meter (AM-350, ADC BioScientific Ltd., UK), and chlorophyll fluorescence was measured using the PlantScreen plant phenotype imaging system. After 30 min of dark adaptation treatment, the chlorophyll fluorescence parameters, including minimum fluorescence after dark adaptation (F_0), maximum photochemical efficiency (F_v/F_m) of photosystem II (PSII) in leaves, photochemical quenching coefficient (qP), and nonphotochemical quenching coefficient (NPQ), were measured using a Chlorophyll Fluorescence Imaging System (FluorCam Photo Systems Instruments, Czech Republic).

Measurement of root exudates and roots

Root exudates. Roots were immersed in 0.2 mmol L^{-1} $CaSO_4$ and 30 mg L^{-1} chloramphenicol solutions for 2 h and 30 min, respectively. Subsequently, the plants were cleaned with sterile deionized water and transferred to a brown glass bottle containing 200 mL of sterile deionized water at 25 °C. After 24 h, 10 mL of solution was taken from each bottle and stored at −20 °C for further metabolic profiling analysis according to Nie *et al*. (2023). The samples were analyzed using gas chromatography-mass spectrometry (Agilent 7890B gas chromatography system and Agilent 5977A MSD system, Agilent Technologies, USA). Separate derivatives using DB-5MS fused silica capillary column (30 m × 0.25 mm × 0.25 μm, Agilent Technologies, USA).

Root aeration tissue. Roots were placed in 2.5% glutaraldehyde fixing solution and fixed in a refrigerator at 4 °C for 24 h, followed by dehydration in a graded ethanol series (30%, 40%, 50%, 60%, and 70%), with each step lasting for 15 min. Slices were cut from the root tip (1 cm) and stained with safranin and solid green. Root aerenchyma was observed using an optical microscope (Nikon Eclipse E100, Nikon, Japan).

Root activity. Roots were weighed. Root activity was determined using the triphenyl tetrazolium chloride (TTC) method (Zhu *et al*., 2020) by a microplate reader (Infinite 200Pro, Tecan Group Ltd., Switzerland).

Root morphology. After 20-d isotope labeling, three rice plants were taken from each treatment. Roots were slowly washed with ultrapure water and scanned with a root scanner (Epson Expression 1680 Scanner, Seiko Epson Corp., Japan). Root morphology indicators were analyzed using the WinRHIZO root analysis system (Regent Instruments Inc., Canada).

Greenhouse gas emission flux measurement

Greenhouse gas emission flux was measured immediately after isotope labeling every 5 d until destructive sampling of plants. Greenhouse gases were collected using a self-made static chamber (100 cm × 50 cm × 85 cm, 0.5 cm thick) between 8:00 and 10:00 a.m. daily. Before gas collection, the static chamber was placed above the soil column and sealed in advance to prevent gas leakage. Then, timing was started, and gas samples were collected at 0, 10, 20, and 30 min while recording the room temperature and the temperature inside the static chamber. After gas sampling, the concentrations of greenhouse gases (CH_4, CO_2, and N_2O) in the gas samples were measured using a high-efficiency gas chromatograph (GC-2014C, Shimadzu Co., Ltd., Japan) within 24 h. The greenhouse gas emission flux (EF, mg m^{-2} h^{-1}) was calculated using the following formula (Wu *et al*., 2009):

$$\mathrm{EF} = \frac{\mathrm{d}c}{\mathrm{d}t} \times \frac{M}{V_0} \times \frac{P}{P_0} \times \frac{T_0}{T} \times H \quad (7)$$

where $\mathrm{d}c/\mathrm{d}t$ (mm^3 m^{-3} h^{-1}) is the slope of the regression curve of the sampled greenhouse gas volume fraction over time, M (g mol^{-1}) is the molar mass of the greenhouse gas, P (Pa) is the pressure inside the static chamber, T_0 (K) is the absolute temperature inside the static chamber (average temperature from the beginning to the end of sampling), V_0 (mL mol^{-1}), P_0 (Pa), and T (K) are the molar volume of gas, atmospheric pressure, and absolute temperature under standard conditions, respectively, and H (m) is the height of the static chamber.

Statistical analysis

Data processing and statistical analysis were conducted using IBM SPSS Statistics 22 and Microsoft Office Excel 2019 software. Graphics were drawn using Origin 2022 software. Differences between different treatments were analyzed using two-way analysis of variance at $P < 0.05$ and Pearson's correlation analysis, while the Duncan's method was used for multiple comparisons.

RESULTS

Rice biomass

After 20 d of pulse labeling, there was no significant difference in the total or shoot biomass of rice plants without AHA application between two irrigation regimes, while the root biomass was significantly higher in DWI0 than in GI0, resulting in a substantially higher root/shoot ratio in DWI0 than in GI0 (Table III). After applying AHA, the total biomass, shoot biomass, and underground biomass of rice plants under two irrigation regimes showed a trend of initial increase and subsequent decrease with the increase in AHA application amount. Among the treatments, DWI3 had the highest biomass in all rice parts, with total biomass, shoot biomass, and root biomass being 16.67%, 6.90%, and 50% higher than GI3, respectively. The DWI6 treatment showed the highest root/shoot ratio of 0.48.

^{13}C in the rice-soil system

After 20 d of pulse labeling, 45.55%–55.36% of assimilated ^{13}C were preserved in rice leaves, 30.85%–36.56% were retained in stems, 5.43%–10.54% were transmitted to roots, and 5.06%–8.64% were transmitted to soil (Table IV). In terms of different irrigation regimes, assimilated ^{13}C remained more in stems and leaves under flooding irrigation, while more assimilated ^{13}C was transported to roots and soil under alternate wetting and drying irrigation. In terms of the amount of AHA application, most assimilated ^{13}C was transferred to roots and soil with AHA application of 300 mg kg^{-1}, especially in DWI3 with the highest assimilated ^{13}C proportion in soil of 8.64%.

Photosynthetic and fluorescence characteristics of rice

Leaf area. Under two irrigation regimes, leaf area

TABLE III

Biomass of rice plants with or without application of artificial humic acid under conventional flooding (GI) or alternate wetting and drying (DWI) irrigation in a $^{13}CO_2$ pulse labeling experiment

Treatment[a)]	Total biomass	Shoot biomass	Root biomass	Root/shoot ratio
	g plant^{-1}			
GI0	1.29 ± 0.05[b)]e[c)]	1.09 ± 0.04c	0.20 ± 0.02f	0.19 ± 0.01e
GI3	2.22 ± 0.02b	1.74 ± 0.02a	0.48 ± 0.01c	0.27 ± 0.01d
GI6	1.65 ± 0.05d	1.26 ± 0.06b	0.39 ± 0.01d	0.31 ± 0.02cd
DWI0	1.30 ± 0.02e	0.97 ± 0.02c	0.34 ± 0.01e	0.35 ± 0.01bc
DWI3	2.59 ± 0.10a	1.86 ± 0.11a	0.72 ± 0.01a	0.39 ± 0.03b
DWI6	2.01 ± 0.02c	1.36 ± 0.01b	0.66 ± 0.01b	0.48 ± 0.01a

[a)] See Table II for the detailed description of each treatment.
[b)] Means ± standard deviations ($n = 6$).
[c)] Means followed by different letters in a column are significantly different at $P < 0.05$.

TABLE IV

^{13}C proportion of each compartment in the total net fixed ^{13}C in the rice-soil system with or without application of artificial humic acid under conventional flooding (GI) or alternate wetting and drying (DWI) irrigation in a $^{13}CO_2$ pulse labeling experiment

Treatment[a)]	^{13}C proportion			
	Leaves	Stems	Roots	Soil
	%			
GI0	52.95 ± 0.16[b)]c[c)]	36.56 ± 0.33a	5.43 ± 0.12f	5.06 ± 0.18d
GI3	50.29 ± 0.24d	33.04 ± 0.24c	9.16 ± 0.13c	7.51 ± 0.17b
GI6	52.45 ± 0.08c	32.79 ± 0.16c	8.39 ± 0.11d	6.37 ± 0.24c
DWI0	53.66 ± 0.24b	31.35 ± 0.33d	9.75 ± 0.11b	5.24 ± 0.21d
DWI3	45.55 ± 0.16e	35.27 ± 0.08b	10.54 ± 0.12a	8.64 ± 0.16a
DWI6	55.36 ± 0.33a	30.85 ± 0.24d	7.36 ± 0.11e	6.43 ± 0.18c

[a)] See Table II for the detailed description of each treatment.
[b)] Means ± standard deviations ($n = 3$).
[c)] Means followed by different letters in a column are significantly different at $P < 0.05$.

gradually increased with the AHA application amount, being the largest in DWI6 (43.10 mm^2) (Fig. 3).

Chlorophyll and Carot concentrations. Under two irrigation regimes, Chl$a$, Chl$b$, and Carot concentrations all showed a gradually increasing trend with the increase of AHA application amount, but there was no significant difference among the treatments (Fig. 3). The DWI6 treatment showed the highest concentrations of Chl$a$ (12.28 mg g^{-1} fresh weight (FW)), Chl$b$ (4.35 mg g^{-1} FW), and Carots (2.18 mg g^{-1} FW).

Rubisco activity. Under both flooding irrigation and alternate wetting and drying irrigation regimes, the Rubisco activity showed a trend of first increasing and then decreasing with the increase of AHA application amount (Fig. 3). The Rubisco activity was the lowest (2.62 μmol g^{-1}FW s^{-1}) in DWI0 and the highest (3.78 μmol g^{-1} FW s^{-1}) in DWI3.

Gas exchange and chlorophyll fluorescence parameters. When AHA was not applied, P_n, T_r, and G_s were higher under alternate wetting and drying irrigation than under flooding irrigation (Fig. 4). At the same time, C_i was lower under alternate wetting and drying irrigation than under flooding irrigation. After AHA application, P_n, T_r, and G_s significantly increased under both irrigation regimes, with the highest values in DWI3, which increased by 65.35%, 33.18%, and 52.58%, respectively, compared to DWI0. However, C_i showed the opposite trend, being the smallest in DWI3, which decreased by 17.18% compared to DWI0.

Overall, the trends of qP and F_v/F_m were similar to that of P_n, while the trends of F_0 and NPQ were opposite (Fig. 4). When AHA was not applied, qP and F_v/F_m were larger in DWI0 than GI0, while F_0 and NPQ were smaller in DWI0 than in GI0. Compared with the absence of AHA, AHA application significantly increased qP and F_v/F_m, while F_0 and NPQ decreased significantly under both irrigation regimes, with the highest qP (0.76) and F_v/F_m (0.78) and the lowest F_0 (290.35) and NPQ (0.05) in DWI3.

Root characteristics

Root exudates. From the perspective of irrigation regimes, the organic acid concentrations were higher under alternate wetting and drying irrigation than under flooding irrigation for the same amount of AHA application (Fig. 5). Under the same irrigation regime, all organic acids showed a trend of first increasing and then decreasing with the increasing AHA application amount. The concentrations of various organic acids were the highest in DWI3 among the treatments, with tartaric acid being the most abundant organic acid, followed by oxalic acid, malic acid, succinic

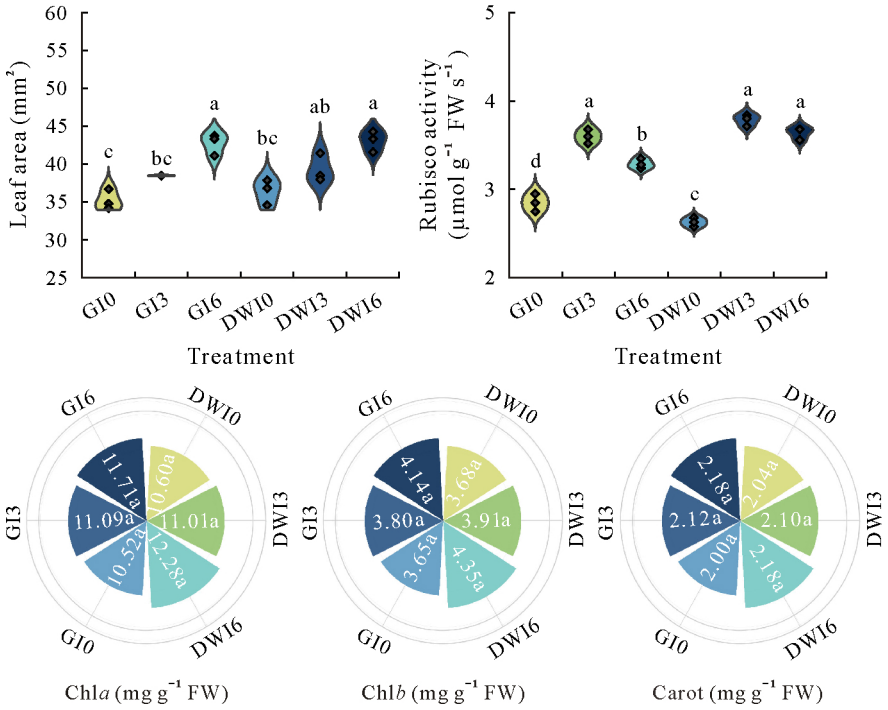

Fig. 3 Violin plots of leaf area and ribulose-1,5-bisphosphate carboxylase/oxygenase (Rubisco) activity and radar charts of chlorophyll *a* (Chl*a*) and *b* (Chl*b*) and carotenoid (Carot) concentrations of rice plants with or without application of artificial humic acid under conventional flooding (GI) or alternate wetting and drying (DWI) irrigation in a $^{13}CO_2$ pulse labeling experiment. See Table II for the detailed description of each treatment. Different letters indicate significant differences at $P < 0.05$. FW = fresh weight.

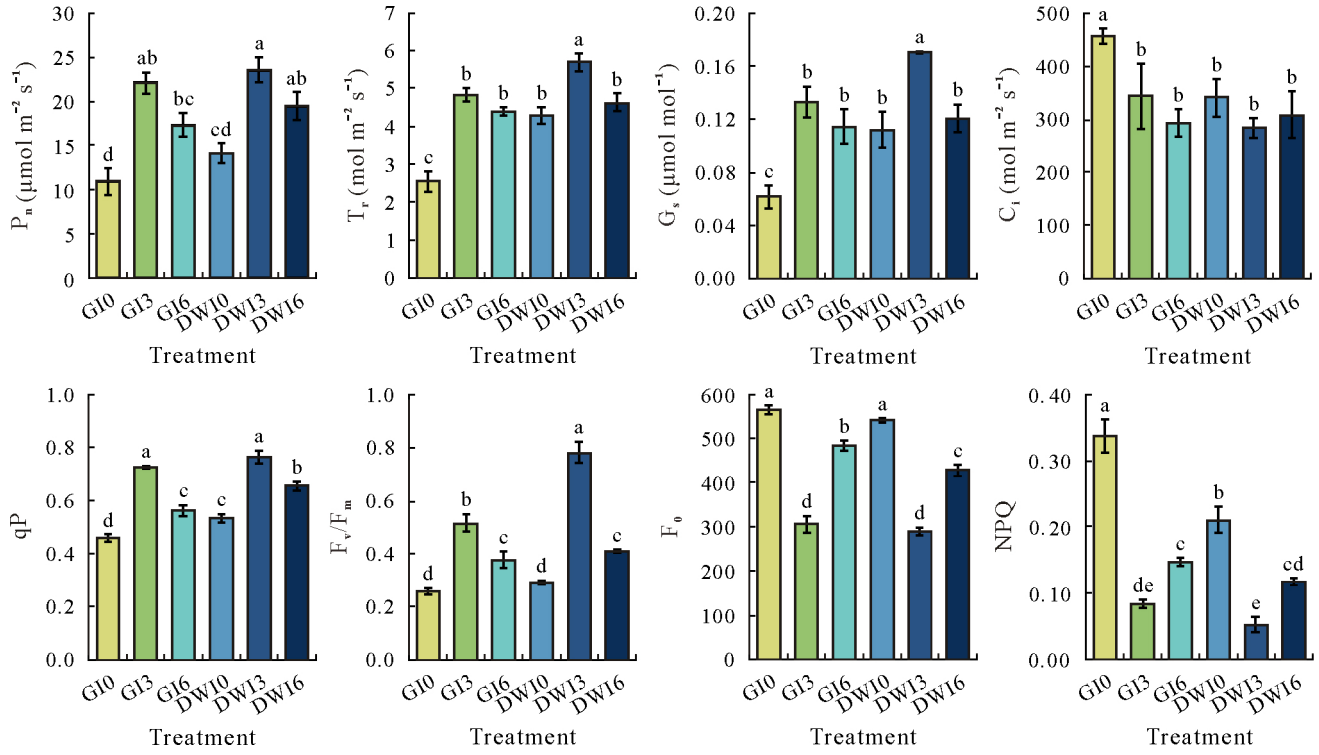

Fig. 4 Gas exchange and chlorophyll fluorescence parameters, including net photosynthetic rate (P_n), transpiration rate (T_r), stomatal conductance (G_s), intercellular CO_2 concentration (C_i), photochemical quenching coefficient (qP), maximum photochemical efficiency (F_v/F_m) of photosystem II in leaves, minimum fluorescence (F_0), and nonphotochemical quenching coefficient (NPQ) of rice plants with or without application of artificial humic acid under conventional flooding (GI) or alternate wetting and drying (DWI) irrigation in a $^{13}CO_2$ pulse labeling experiment. See Table II for the detailed description of each treatment. Error bars are standard deviations of means ($n = 6$). Different letters above the bars indicate significant differences at $P < 0.05$.

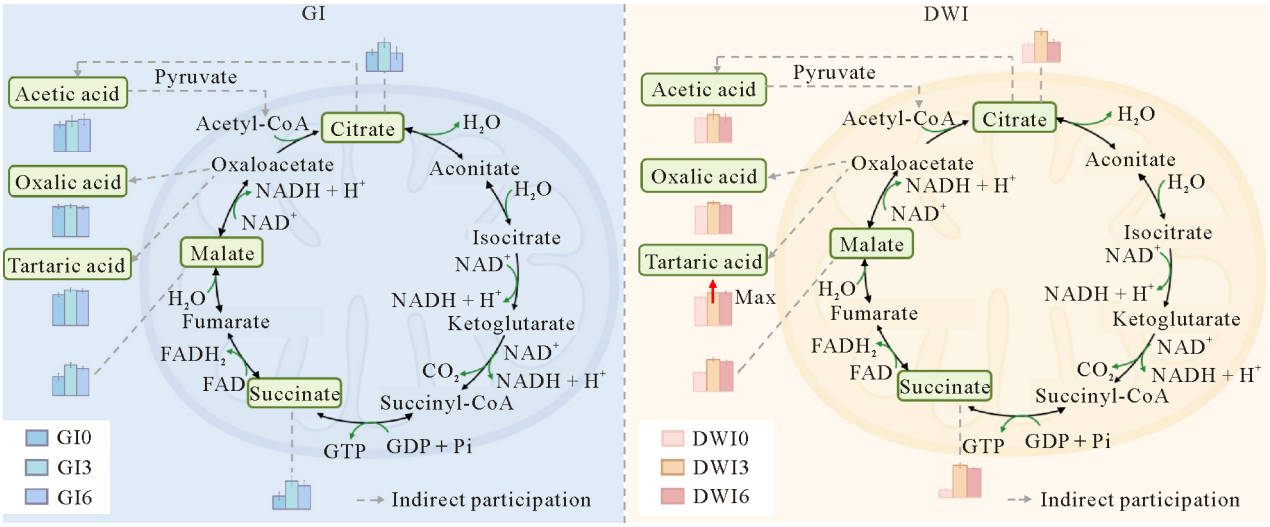

Fig. 5 Concentrations of organic acids in root exudates of rice plants with or without application of artificial humic acid under conventional flooding (GI) or alternate wetting and drying (DWI) irrigation in a $^{13}CO_2$ pulse labeling experiment. See Table II for the detailed description of each treatment. $FADH_2$ = flavin adenine dinucleotide; FAD = flavin adenine dinucleotide; GTP = guanosine triphosphate; GDP = guanosine diphosphate; Pi = inorganic P; CoA = coenzyme A; NADH and NAD^+ = reduced and oxidized forms of nicotinamide adenine dinucleotide, respectively; Max = maximum.

acid, citric acid, and acetic acid. They increased by 13.08%, 10.41%, 47.66%, 108.66%, 24.37%, and 6.06% in DWI3, respectively, compared with DWI0.

Root morphology. From the perspective of irrigation regimes, root length, surface area, and length density of rice were all higher under alternate wetting and drying irrigation than those under flooding irrigation (Fig. 6). Under flooding irrigation, AHA application significantly increased the surface area, length, and length density of roots, with the most pronounced effect on root length density at the depth of 20–40 cm. However, there was no statistically significant difference caused by different AHA application amounts. Under alternate wetting and drying irrigation, the application of AHA significantly increased root length and length density, with a more significant promoting effect of DWI3 than DWI6. Compared with DWI0, the root length and length density increased by 23.60% and 25.44% in DWI3, respectively.

Root aeration tissue. When AHA was not applied, rice roots produced aerated tissue under two irrigation regimes, with more aerated tissue under flooding irrigation compared to alternate wetting and drying irrigation (Fig. 6b). As the AHA application amount increased, the amount of aerated tissue gradually decreased under flooding irrigation. However, no aeration tissue was generated during alternate wetting and drying irrigation.

Root activity. When AHA was not applied, root activity was significantly higher in DWI0 than in GI0 (Fig. 6e). After AHA application, root activities in DWI3 and DWI6 were significantly higher than those in GI3 and GI6, respectively, with the highest value in DWI3 (601.71 μg TTC g^{-1} h^{-1}).

Greenhouse gas emission

Irrigation regimes and AHA application amounts did not significantly impact N_2O emission (Fig. 6f). When AHA was not applied, DWI0 significantly reduced CH_4 emission flux but increased CO_2 emission flux compared to GI0 (Fig. 6g, h). The impact of AHA application on CH_4 and CO_2 emissions was the greatest in GI3 and DWI3. Among the treatments, CH_4 emission flux was the lowest in DWI3, decreasing by 13.72% compared to DWI0, and CO_2 emission flux was the lowest in GI3, GI6, and DWI3, with no significant difference among these three treatments.

Correlation analysis

Pearson's correlation analysis showed that the leaf ^{13}C content was significantly positively correlated with total biomass, and the root ^{13}C content was significantly positively correlated with root surface area. Soil ^{13}C content was significantly positively correlated with P_n and total biomass (Mantel's $P < 0.01$) and positively correlated with Rubisco activity, root length, and root activity (Mantel's $P < 0.05$) (Fig. 7).

DISCUSSION

Effect of AHA application on photosynthetic C fixation in rice under two irrigation regimes

Rice fixes CO_2 in the atmosphere into organic matter through photosynthesis, and the photosynthetic efficiency directly affects soil C cycling (Liu Z W *et al.*, 2021). Under two irrigation regimes, AHA application increased leaf area, Chl*a*, Chl*b*, and Carot concentrations, and Rubisco

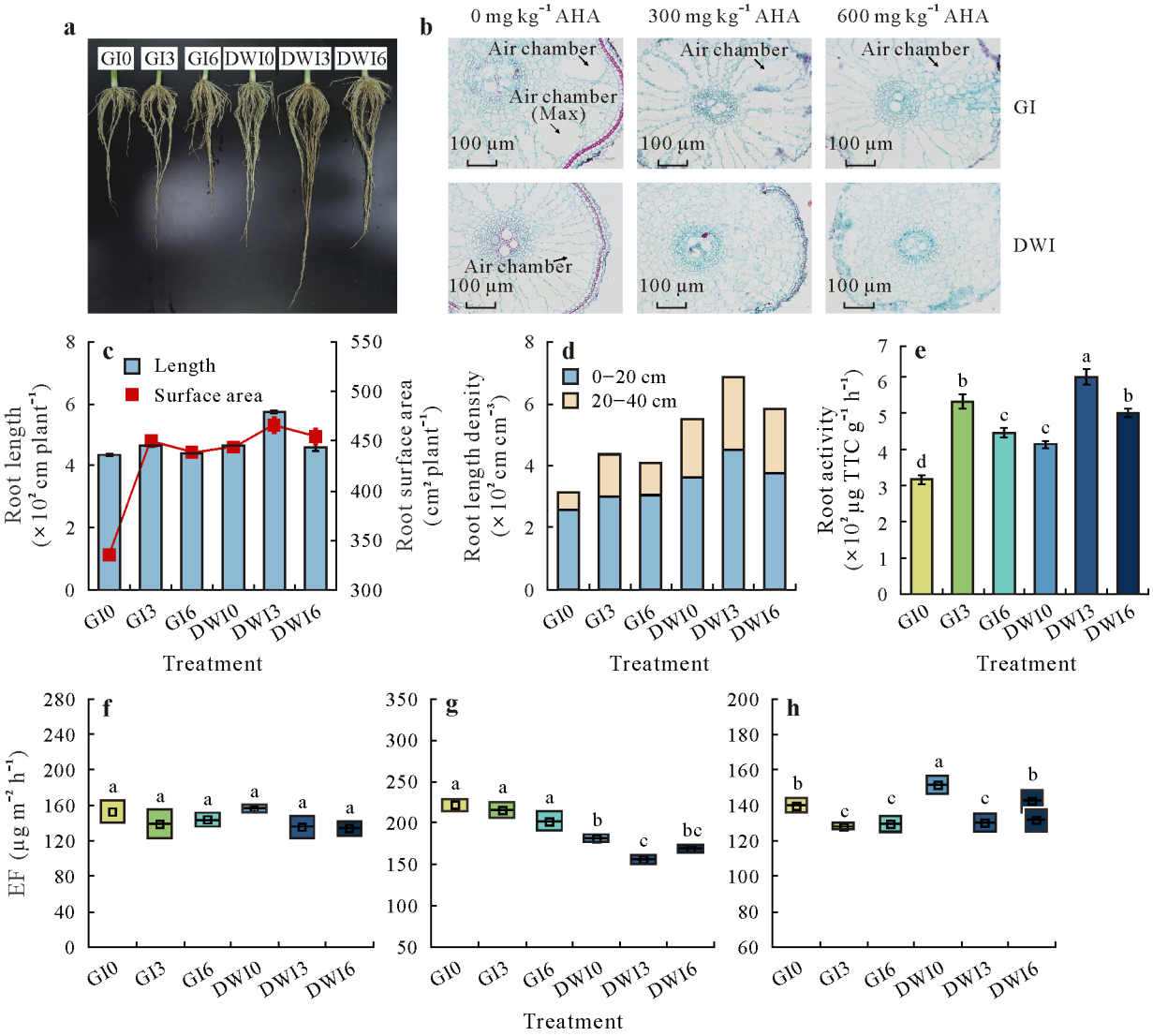

Fig. 6 Root morphology (a), aeration tissue (b), length and surface area (c), length density (d), and activity (e) of rice plants, and box plots of emission fluxes (EF) of greenhouse gases, including N_2O (f), CH_4 (g), and CO_2 (h), in the rice-soil system with or without application of artificial humic acid (AHA) under conventional flooding (GI) or alternate wetting and drying (DWI) irrigation in a $^{13}CO_2$ pulse labeling experiment. See Table II for the detailed description of each treatment. TTC = triphenyl tetrazolium chloride; Max = maximum. In panels c and e, error bars are standard deviations of means ($n = 6$). In panels e–h, different letters indicate significant differences at $P < 0.05$.

activity compared to the absence of AHA (Fig. 3). This indicates that AHA application could enhance rice light-harvesting ability, antioxidant capacity, and CO_2 assimilation ability by promoting the growth of rice leaves, as well as the absorption and utilization of nutrients, and improving the photosynthetic efficiency of rice, thereby increasing rice P_n. However, with the increase in AHA application amount, the leaf Chl*a* and Chl*b* concentrations and leaf area gradually increased. In contrast, leaf P_n, T_r, G_s, and Rubisco activity first increased and then decreased, while the C_i concentration first decreased and then increased. Light was more easily transmitted through the leaves with AHA application of 300 mg kg^{-1}, perhaps due to the moderate leaf size, resulting in an increase in light transmittance in the middle and lower parts of the plant, which increases light absorption in the lower leaves and is beneficial for plant photosynthesis (de Castro and Fetcher, 1999). At the same time, increased stomatal conductance helps more CO_2 enter the leaves for photosynthesis and promotes water transpiration, effectively dissipating heat and maintaining water balance through transpiration (Katul *et al.*, 2010). The decrease in intercellular CO_2 concentration indicates that the CO_2 supply is sufficient during photosynthesis, and due to the high activity of leaf photosynthetic enzymes, the CO_2 entering the leaves can be effectively utilized for photosynthesis (Li *et al.*, 2015). With the AHA application of 600 mg kg^{-1}, the light energy absorbed by rice may far exceed the physiological metabolic requirement, and there is a redundancy phenomenon in leaf chlorophyll concentrations. The upper leaves are relatively large, making it difficult for

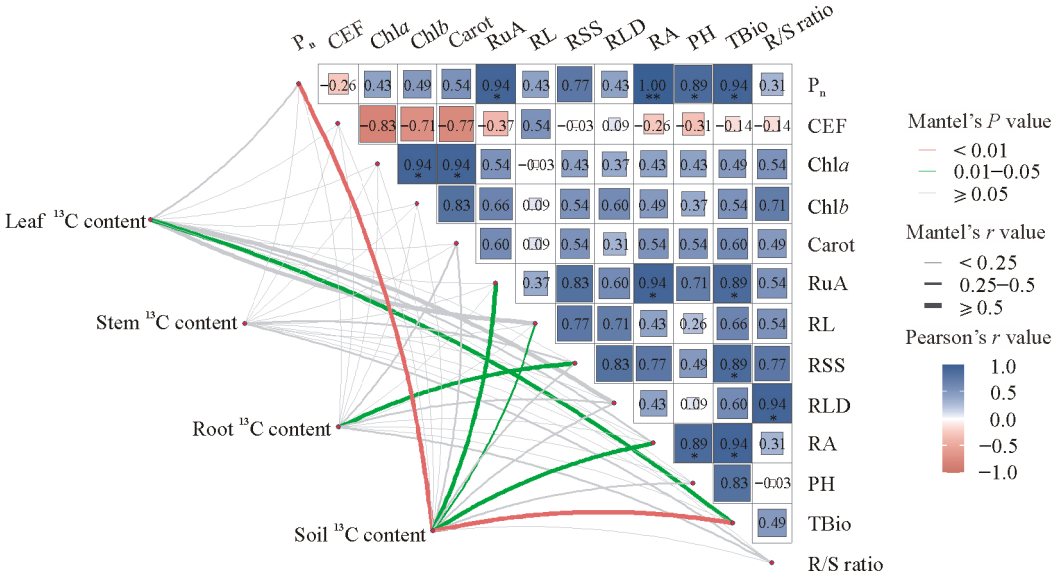

Fig. 7 Correlations of ^{13}C contents in leaves, stems, roots, and soil with photosynthetic indicators, including net photosynthetic rate (P_n), CO_2 emission flux (CEF), chlorophyll *a* and b (Chl*a* and Chl*b*, respectively) and carotenoid (Carot) concentrations, and ribulose-1,5-bisphosphate carboxylase/oxygenase (Rubisco) activity (RuA), and plant indicators, including root length (RL), root surface area (RSS), root length density (RLD), root activity (RA), plant height (PH), total biomass (TBio), and root/shoot (R/S) ratio. Asterisks * and ** indicate significant correlations at $P < 0.05$ and $P < 0.01$, respectively.

light to penetrate the lower leaves, suppressing the absorption of light energy by the lower leaves, and ultimately reducing the photosynthetic rate.

The chlorophyll fluorescence parameter was obtained by measuring the fluorescence released by chlorophyll molecules after absorbing light energy. The intensity and characteristics of fluorescence can reflect the efficiency of PSII and the photochemical state of plants (Zeng *et al.*, 2016). In this study, without applying AHA, the F_v/F_m and qP were larger in DWI0 than in GI0, while F_0 and NPQ were smaller in DWI0 than in GI0 (Fig. 4). The F_v/F_m and qP were higher under alternate wetting and drying irrigation than under flooding irrigation, indicating that plants adapt to environmental changes by improving the efficiency of PSII and photochemical processes under alternate wetting and drying irrigation, thereby maximizing the utilization of light energy under limited water condition, which is similar to Mielke and Schaffer (2010). The F_0 is related to the open state of the PSII reaction center (Baghbani-Arani *et al.*, 2017). The decrease in F_0 may indicate that the reaction center of PSII is more stable after dark adaptation or that the repair mechanism of PSII is more effective under alternate wetting and drying irrigation, reducing the open state of the reaction center and thus reducing fluorescence production. The NPQ is an indicator for measuring nonphotochemical quenching processes, reflecting the ability of plants to regulate excess light energy through nonphotochemical processes such as heat dissipation (Berne *et al.*, 2018). The increase in NPQ is usually related to the light protection mechanism of plants, indicating that plants can more effectively dissipate energy in the face of excessive light energy to avoid light damage. Under alternate wetting and drying irrigation, a decrease in NPQ may indicate that plants have reduced their dependence on heat dissipation and more effectively utilize light energy. In treatments with AHA application, F_v/F_m and qP were the highest, while F_0 and NPQ were the lowest in DWI3. It indicates that the photosynthetic performance of PSII is enhanced rather than dissipated in DWI3. This is because AHA can improve soil structure, provide a suitable micro-environment, increase soil water and fertilizer retention capacity, and promote plant absorption and utilization of nutrients. Meanwhile, moderate water stress generated by alternate wetting and drying irrigation can promote the development of plant roots, enhance the absorption capacity of plants for water and nutrients, increase the chlorophyll concentrations, P_n, and F_v/F_m (Luo *et al.*, 2016; Song *et al.*, 2019). The coupling of AHA and alternate wetting and drying irrigation produced a synergistic effect, further improving the photosynthetic efficiency of rice. The comprehensive analyses of rice gas exchange parameters and chlorophyll fluorescence parameters showed that the DWI3 treatment had the highest photosynthetic efficiency and the strongest photosynthetic C sequestration ability among all treatments.

Effect of AHA application on C transfer in rice roots under two irrigation regimes

Roots are the main crop organ that absorbs water and nutrients and the leading site for synthesizing various organic acids (Wen *et al.*, 2022). Root morphology, biomass, and exudates are essential indicators for evaluating the C transport capacity of roots (Wang *et al.*, 2019). When AHA

was not applied, alternate wetting and drying irrigation promoted root growth, resulting in a significant increase in root biomass, length, surface area, and length density, compared to flooding irrigation (Table III, Fig. 6c, d). Under alternate wetting and drying irrigation, rice roots underwent more frequent water stress and rehydration processes. This periodic water change stimulated root growth and renewal, thereby enhancing root metabolic activity and vitality (Figs. 5 and 6e), helping to improve root absorption of water and nutrients, and promoting the synthesis and release of root exudates (Zhang *et al*., 2013). Under flooding irrigation, long-term water saturation could lead to insufficient oxygen supply, affecting root activity; however, the aeration tissue of rice roots was more developed than those under alternate wetting and drying irrigation (Fig. 6b). The reason is that under flooding irrigation, rice roots are in an anaerobic environment saturated with water for a long time, causing the air cavity to expand and forming a continuous gas channel, allowing oxygen to be transported from the soil surface to the deeper parts of the roots to improve the efficiency of oxygen acquisition and transportation. In contrast, under alternate wetting and drying irrigation, periodic drainage can allow oxygen to enter soil, and rice can rely on the natural diffusion of oxygen in soil to meet its needs. Therefore, the aeration tissue is less developed under alternate wetting and drying irrigation than under flooded irrigation.

The organic acids in root exudates are products of plant root metabolic activity. These organic acids can be synthesized in plants through metabolic pathways, such as the tricarboxylic acid cycle, or generated from other metabolites through specific enzymatic reactions (Canarini *et al*., 2019). The application of AHA increased the concentrations of organic acids such as citric acid, tartaric acid, oxalic acid, and acetic acid in rice root exudates (Fig. 5). Organic acids can interact with minerals in soil. This contributes to the formation and stability of soil structure, thereby affecting the fixation and preservation of organic C in soil (Adeleke *et al*., 2017). Meanwhile, organic acids help regulate rhizosphere pH, affecting the form of nutrients in soil and the absorption efficiency of plants, thereby promoting root growth (Wang and Tang, 2018). Although the application of AHA under the two irrigation conditions in this study may have adverse effects on the oxygen supply of roots by reducing root aeration tissue, the increase in root activity indicates that rice can still maintain an excellent physiological state under these conditions (Fig. 6b, e), suggesting that the application of AHA improves soil aeration. Under the same amount of AHA application, AHA had better effects on rice root biomass, root morphology indicators, and organic acid secretion under alternate wetting and drying irrigation than under flooding irrigation, especially in DWI3 (Table III, Figs. 5 and 6c, d). The reason is that AHA changes the viscosity and surface tension of pore fluid in soil, increases soil water retention capacity, and reduces soil saturated hydraulic conductivity, thus benefiting root growth and vitality (Yang *et al*., 2020). At the same time, alternate wetting and drying irrigation improves soil permeability and oxygen supply, helping to increase nutrient effectiveness and promote root absorption efficiency. However, excessive AHA concentration may lead to excessive nutrient supply in soil, causing nutrient imbalance and affecting the normal development of roots, negatively impacting root activity (Liu *et al*., 2019; Zhang, 2021).

Effect of AHA application on greenhouse gas emissions under two irrigation regimes

Part of the organic C fixed in soil is released into the atmosphere through greenhouse gases such as CO_2 and CH_4, which is an essential pathway for SOC loss (van Groenigen *et al*., 2011). In this study, when AHA was not applied, alternate wetting and drying irrigation significantly reduced CH_4 emission flux and promoted CO_2 emission flux but had no significant effect on N_2O emission flux (Fig. 6f–h). Paddy soils remain in a saturated water state for a long time under flooding irrigation, forming an anaerobic environment that facilitates the activity of methane-producing bacteria, thereby promoting the production and emission of CH_4. Alternate wetting and drying irrigation breaks this anaerobic condition, increasing soil aeration through periodic drainage and re-flooding, promoting root respiration, and inhibiting the activity of methanogenic bacteria, thereby reducing CH_4 production and increasing CO_2 production and emission (Sander *et al*., 2020). In addition, the production of N_2O is related to nitrification and denitrification in soil. Alternate wetting and drying irrigation may inhibit nitrification by reducing water supply, while promoting denitrification by increasing soil aeration. This mutual offsetting effect may result in no significant change in N_2O emission flux (Lewicka-Szczebak *et al*., 2016).

When AHA was applied, DWI6 did not significantly affect CH_4, while DWI3 significantly reduced CH_4 emission (Fig. 6g). The reason is that under alternate wetting and drying irrigation, soil undergoes periodic oxidation and reduction processes. At the same time, AHA application may increase the organic matter content in soil, thereby promoting CH_4 oxidation during the oxidation stage. Especially at moderate amount (300 mg kg^{-1}), AHA application may provide suitable C sources and electron acceptors, enhance methane oxidation, and significantly reduce CH_4 emissions. The AHA application at a high amount (600 mg kg^{-1}) may lead to excess C sources in soil, leading to increased competitive soil microbial activity, and thus inhibiting the oxidation process of CH_4 (Tan *et al*., 2018). In addition, under both irrigation regimes, AHA application significantly

reduced CO_2 emission flux, with the lowest CO_2 emission flux in GI3 (Fig. 6h), which may be due to the improved soil structure and increased soil porosity. This helps to increase the oxygen concentration in soil, thereby inhibiting the activity of anaerobic microorganisms and reducing CO_2 production. However, AHA application of 600 mg kg^{-1} may lead to excess C sources, affecting the metabolic balance of microorganisms. Therefore, AHA application showed more effect on reducing CO_2 emission at 600 mg kg^{-1} than at 300 mg kg^{-1} AHA. Except for GI3, the CO_2 emission flux was also lower under GI6 and DIW3 among the treatments, and there was no significant difference among the three treatments. However, AHA application did not significantly impact N_2O emission flux under both irrigation regimes (Fig. 6f). The application of AHA may affect the activities of nitrifying and denitrifying bacteria in soil. However, the enhancement of nitrification was equivalent to the enhancement of denitrification. Therefore, there was no significant change in N_2O emission. Overall, the CH_4, CO_2, and N_2O emission fluxes were relatively low in DWI3, indicating less SOC loss.

Effect of AHA application on photosynthetic C allocation under two irrigation regimes

Overall, the distribution ratio of ^{13}C in various parts of rice and soil was ranked in the order of leaves $>$ stems $>$ roots $>$ soil, indicating that ^{13}C was more retained in the aboveground parts, which was similar to Liu *et al*. (2023). From the perspective of irrigation regimes, under the same amount of AHA application, alternate wetting and drying irrigation transferred more ^{13}C to the underground compared with flooding irrigation, and with the increase of AHA application, the ^{13}C content in the underground showed a trend of first increasing and then decreasing. According to the correlation analysis (Fig. 7), the ^{13}C content in soil had extremely significant positive correlations with P_n and total biomass and significant positive correlations with Rubisco activity, root activity, and root length, indicating that the ability of photosynthesis to fix C and the root ability to transport C jointly affect the content of ^{13}C in soil. This is because plants fix CO_2 in the atmosphere through photosynthesis, convert it into organic matter, and store it in the plant body while transporting and releasing part of organic C into soil through roots. Therefore, improving the photosynthetic capacity and root ability of plants to transport C can significantly enhance soil C sequestration capacity. Among the treatments, the ^{13}C content in soil was the maximum in DWI3, due to the greater SOC sequestration caused by the strongest photosynthetic capacity, the most potent C transport ability of roots, and lower greenhouse gas emission fluxes in DWI3.

CONCLUSIONS

Under alternate wetting and drying irrigation with AHA application, from the perspective of photosynthetic C sequestration, the increases in Chl*a*, Chl*b*, and Carot concentrations and Rubisco activity led to an improvement in leaf photosynthetic capacity. In terms of roots, the enhanced aeration tissue and root activity, the increased concentrations of various organic acids in root exudates, and the increased root biomass promoted the ability of C transport of roots. Regarding greenhouse gas emissions, both CH_4 and CO_2 emissions significantly decreased, reducing the loss of organic C. However, attention should be paid to the appropriate AHA application amount. Among the treatments, DWI3 showed the maximal photosynthetic C sequestration capacity and transport capacity of roots and lowest greenhouse gas emission flux. Therefore, DWI3 was regarded as a recommended management practice for C sequestration and water conservation in the rice-soil system.

DECLARATION OF COMPETING INTEREST

The authors declare that they have no known competing financial interests or personal relationships that could have appeared to influence the work reported in this paper.

ACKNOWLEDGEMENT

The authors appreciate the financial support of the National Key Research and Development Program of China (No. 2022YFD1500100), the National Natural Science Foundation of China (No. 52279034), the Opening Project of International Cooperation Joint Laboratory of Health in Cold Region Black Soil Habitat of the Ministry of Education, China (No. HCRBSH202311-03), the Key Laboratory of Germplasm Innovation and Physiological Ecology of Cold land Grain Crops, Ministry of Education, China (No. CXSTOP202304).

REFERENCES

Adeleke R, Nwangburuka C, Oboirien B. 2017. Origins, roles and fate of organic acids in soils: A review. *S Afr J Bot*. **108**: 393–406.

Ainsworth E A, Bush D R. 2011. Carbohydrate export from the leaf: A highly regulated process and target to enhance photosynthesis and productivity. *Plant Physiol*. **155**: 64–69.

Alavaisha E, Tumbo M, Senyangwa J, Mourice, S. 2022. Influence of water management farming practices on soil organic carbon and nutrients: A case study of rice farming in Kilombero Valley, Tanzania. *Agronomy*. **12**: 1148.

Baghbani-Arani A, Modarres-Sanavy S A M, Mashhadi-Akbar-Boojar M, Mokhtassi-Bidgoli A. 2017. Towards improving the agronomic performance, chlorophyll fluorescence parameters and pigments in fenugreek using zeolite and vermicompost under deficit water stress. *Ind Crops Prod*. **109**: 346–357.

Berne N, Fabryova T, Istaz B, Cardol P, Bailleul B. 2018. The peculiar NPQ regulation in the stramenopile *Phaeomonas* sp. challenges the xanthophyll cycle dogma. *Biochim Biophys Acta* (*BBA*) *Bioenerg*. **1859**: 491–500.

Canarini A, Kaiser C, Merchant A, Richter A, Wanek W. 2019. Root exudation of primary metabolites: Mechanisms and their roles in plant responses to environmental stimuli. *Front Plant Sci*. **10**: 157.

Carrijo D R, Lundy M E, Linquist B A. 2017. Rice yields and water use under alternate wetting and drying irrigation: A meta-analysis. *Field Crops Res*. **203**: 173–180.

Chen X B, Hu Y J, Xia Y H, Zheng S M, Ma C, Rui Y C, He H B, Huang D Y, Zhang Z H, Ge T D, Wu J S, Guggenberger G, Kuzyakov Y, Su Y R. 2021. Contrasting pathways of carbon sequestration in paddy and upland soils. *Glob Change Biol*. **27**: 2478–2490.

de Castro F, Fetcher N. 1999. The effect of leaf clustering in the interception of light in vegetal canopies: Theoretical considerations. *Ecol Model*. **116**: 125–134.

De Pessemier J, Moturu T R, Nacry P, Ebert R, De Gernier H, Tillard P, Swarup K, Wells D M, Haseloff J, Murray S C, Bennett M J, Inzé D, Vincent C I, Hermans C. 2022. Root system size and root hair length are key phenes for nitrate acquisition and biomass production across natural variation in Arabidopsis. *J Exp Bot*. **73**: 3569–3583.

Dodd I C, Puértolas J, Huber K, Pérez-Pérez J G, Wright H R, Blackwell M S A. 2015. The importance of soil drying and re-wetting in crop phytohormonal and nutritional responses to deficit irrigation. *J Exp Bot*. **66**: 2239–2252.

Du Q, Zhang S S, Song J P, Zhao Y, Yang F. 2020. Activation of porous magnetized biochar by artificial humic acid for effective removal of lead ions. *J Hazard Mater*. **389**: 122115.

Gayathri R, Mahboob S, Govindarajan M, Al-Ghanim K A, Ahmed Z, Al-Mulahim N, Vodovnik M, Vijayalakshmi S. 2021. A review on biological carbon sequestration: A sustainable solution for a cleaner air environment, less pollution and lower health risks. *J King Saud Univ Sci*. **33**: 101282.

Ge T D, Yuan H Z, Zhu H H, Wu X H, Nie S A, Liu C, Tong C L, Wu J S, Brookes P. 2012. Biological carbon assimilation and dynamics in a flooded rice-soil system. *Soil Biol Biochem*. **48**: 39–46.

Grunwald D, Kaiser M, Piepho H P, Koch H J, Rauber R, Ludwig B. 2018. Effects of biochar and slurry application as well as drying and rewetting on soil macro-aggregate formation in agricultural silty loam soils. *Soil Use Manage*. **34**: 575–583.

Gujjar R S, Banyen P, Chuekong W, Worakan P, Roytrakul S, Supaibulwatana K. 2020. A synthetic cytokinin improves photosynthesis in rice under drought stress by modulating the abundance of proteins related to stomatal conductance, chlorophyll contents, and Rubisco activity. *Plants*. **9**: 1106.

Harman G E, Doni F, Khadka R B, Uphoff N. 2021. Endophytic strains of *Trichoderma* increase plants' photosynthetic capability. *J Appl Microbiol*. **130**: 529–546.

Huang Q N, Wu Y L, Shao G S. 2021. Root aeration promotes cadmium accumulation in rice by regulating iron uptake-associated system. *Rice Sci*. **28**: 511–520.

Jansson C, Wullschleger S D, Kalluri U C, Tuskan G A. 2010. Phytosequestration: Carbon biosequestration by plants and the prospects of genetic engineering. *BioScience*. **60**: 685–696.

Katul G, Manzoni S, Palmroth S, Oren R. 2010. A stomatal optimization theory to describe the effects of atmospheric CO_2 on leaf photosynthesis and transpiration. *Ann Bot*. **105**: 431–442.

Kuzyakov Y, Schneckenberger K. 2004. Review of estimation of plant rhizodeposition and their contribution to soil organic matter formation. *Arch Agron Soil Sci*. **50**: 115–132.

Lei X, Shen Y T, Zhao J N, Huang J J, Wang H, Yu Y, Xiao C W. 2023. Root exudates mediate the processes of soil organic carbon input and efflux. *Plants*. **12**: 630.

Lewicka-Szczebak D, Dyckmans J, Kaiser J, Marca A, Augustin J, Well R. 2016. Oxygen isotope fractionation during N_2O production by soil denitrification. *Biogeosciences*. **13**: 1129–1144.

Li H D, Wang Y, Xiao J, Xu K. 2015. Reduced photosynthetic dark reaction triggered by ABA application increases intercellular CO_2 concentration, generates H_2O_2 and promotes closure of stomata in ginger leaves. *Environ Exp Bot*. **113**: 11–17.

Liao B, Wu X, Yu Y F, Luo S Y, Hu R G, Lu G A. 2020. Effects of mild alternate wetting and drying irrigation and mid-season drainage on CH_4 and N_2O emissions in rice cultivation. *Sci Total Environ*. **698**: 134212.

Liu Y L, Ge T D, van Groenigen K J, Yang Y H, Wang P, Cheng K, Zhu Z K, Wang J K, Li Y, Guggenberger G, Sardans J, Penuelas J, Wu J S, Kuzyakov Y. 2021. Rice paddy soils are a quantitatively important carbon store according to a global synthesis. *Commun Earth Environ*. **2**: 154.

Liu Y L, Ge T D, Zhu Z K, Liu S L, Luo Y, Li Y, Wang P, Gavrichkova O, Xu X L, Wang J K, Wu J S, Guggenberger G, Kuzyakov Y. 2019. Carbon input and allocation by rice into paddy soils: A review. *Soil Biol Biochem*. **133**: 97–107.

Liu Z Q, Su Z J, Chen J Y, Zou J Y, Liu Z X, Li Y Z, Wang J, Wu L Z, Wei H, Zhang J E. 2023. Polyethylene microplastics can attenuate soil carbon sequestration by reducing plant photosynthetic carbon assimilation and transfer: Evidence from a ^{13}C-labeling mesocosm study. *J Clean Prod*. **385**: 135558.

Liu Z W, Wu X L, Li S X, Liu W, Bian R J, Zhang X H, Zheng J F, Drosos M, Li L Q, Pan G X. 2021. Quantitative assessment of the effects of biochar amendment on photosynthetic carbon assimilation and dynamics in a rice-soil system. *New Phytol*. **232**: 1250–1258.

Luo H H, Zhang Y L, Zhang W F. 2016. Effects of water stress and rewatering on photosynthesis, root activity, and yield of cotton with drip irrigation under mulch. *Photosynthetica*. **54**: 65–73.

Martínez-Alcántara B, Jover S, Quiñones A, Forner-Giner M Á, Rodríguez-Gamir J, Legaz F, Primo-Millo E, Iglesias D J. 2012. Flooding affects uptake and distribution of carbon and nitrogen in citrus seedlings. *J Plant Physiol*. **169**: 1150–1157.

Mielke M S, Schaffer B. 2010. Leaf gas exchange, chlorophyll fluorescence and pigment indexes of *Eugenia uniflora* L. in response to changes in light intensity and soil flooding. *Tree Physiol*. **30**: 45–55.

Ministry of Water Resources of the People's Republic of China (MWR). 2020. China Water Resources Bulletin 2019 (in Chinese). China Water Resources and Hydropower Press, Beijing.

Nie Z J, Wang L L, Zhao P, Wang Z B, Shi Q Z, Liu H G. 2023. Metabolomics reveals the impact of nitrogen combined with the zinc supply on zinc availability in calcareous soil *via* root exudates of winter wheat (*Triticum aestivum*). *Plant Physiol Biochem*. **204**: 108069.

Runkle B R K, Suvočarev K, Reba M L, Reavis C W, Smith S F, Chiu Y L, Fong B. 2019. Methane emission reductions from the alternate wetting and drying of rice fields detected using the eddy covariance method. *Environ Sci Technol*. **53**: 671–681.

Salvucci M E. 1989. Regulation of Rubisco activity *in vivo*. *Physiol Plant*. **77**: 164–171.

Sander B O, Schneider P, Romasanta R, Samoy-Pascual K, Sibayan E B, Asis C A, Wassmann R. 2020. Potential of alternate wetting and drying irrigation practices for the mitigation of GHG emissions from rice fields: Two cases in Central Luzon (Philippines). *Agriculture*. **10**: 350.

Sasse J. 2023. Plant chemistry and morphological considerations for efficient carbon sequestration. *Chimia*. **77**: 726–732.

Sidhu G K, Nogia P, Tomar V, Mehrotra R, Mehrotra S. 2021. *In vitro* activity of reconstituted Rubisco enzyme from *Gloeobacter violaceus*. *J Biosci*. **46**: 67.

Song T, Xu F Y, Yuan W, Chen M X, Hu Q J, Tian Y, Zhang J H, Xu W F. 2019. Combining alternate wetting and drying irrigation with reduced phosphorus fertilizer application reduces water use and promotes phosphorus use efficiency without yield loss in rice plants. *Agric Water Manage*. **223**: 105686.

Tan W B, Jia Y F, Huang C H, Zhang H, Li D, Zhao X Y, Wang G A, Jiang J, Xi B D. 2018. Increased suppression of methane production by humic substances in response to warming in anoxic environments. *J Environ Manage*. **206**: 602–606.

Tang C Y, Cheng K, Liu B L, Antonietti M, Yang F. 2022. Artificial humic acid facilitates biological carbon sequestration under freezing-thawing conditions. *Sci Total Environ*. **849**: 157841.

Tang L L, Zhan M, Shang C H, Yuan J Y, Wan Y B, Qin M G. 2021. Dynamics of root exuded carbon and its relationships with root traits of rapeseed and wheat. *Plant Soil Environ*. **67**: 317–323.

Tian X P, Wang L, Hou Y H, Wang H, Tsang Y F, Wu J H. 2019. Responses of soil microbial community structure and activity to incorporation of straws and straw biochars and their effects on soil respiration and soil organic carbon turnover. *Pedosphere*. **29**: 492–503.

van Groenigen K J, Osenberg C W, Hungate B A. 2011. Increased soil emissions of potent greenhouse gases under increased atmospheric CO_2. *Nature*. **475**: 214–216.

Vives-Peris V, de Ollas C, Gómez-Cádenas A, Pérez-Clemente R M. 2020. Root exudates: From plant to rhizosphere and beyond. *Plant Cell Rep*. **39**: 3–17.

Wang D Y, Felice M L, Scow K M. 2020. Impacts and interactions of biochar and biosolids on agricultural soil microbial communities during dry and wet-dry cycles. *Appl Soil Ecol*. **152**: 103570.

Wang J S, Defrenne C, McCormack M L, Yang L, Tian D S, Luo Y Q, Hou E Q, Yan T, Li Z L, Bu W S, Chen Y, Niu S L. 2021. Fine-root functional trait responses to experimental warming: A global meta-analysis. *New Phytol*. **230**: 1856–1867.

Wang R Z, Bicharanloo B, Shirvan M B, Cavagnaro T R, Jiang Y, Keitel C, Dijkstra F A. 2021. A novel ^{13}C pulse-labelling method to quantify the contribution of rhizodeposits to soil respiration in a grassland exposed to drought and nitrogen addition. *New Phytol*. **230**: 857–866.

Wang X J, Tang C X. 2018. The role of rhizosphere pH in regulating the rhizosphere priming effect and implications for the availability of soil-derived nitrogen to plants. *Ann Bot*. **121**: 143–151.

Wang Y N, Gao G Q, Wang N, Wang Z Q, Gu J C. 2019. Effects of morphology and stand structure on root biomass and length differed between absorptive and transport roots in temperate trees. *Plant Soil*. **442**: 355–367.

Wen Z H, White P J, Shen J B, Lambers H. 2022. Linking root exudation to belowground economic traits for resource acquisition. *New Phytol*. **233**: 1620–1635.

Whalen J K, Gul S, Poirier V, Yanni S F, Simpson M J, Clemente J S, Feng X J, Grayston S J, Barker J, Gregorich E G, Angers D A, Rochette P, Janzen H H. 2014. Transforming plant carbon into soil carbon: Process-level controls on carbon sequestration. *Can J Plant Sci*. **94**: 1065–1073.

Wu J, Zhang J, Jia W L, Xie H J, Gu R R, Li C, Gao B Y. 2009. Impact of COD/N ratio on nitrous oxide emission from microcosm wetlands and their performance in removing nitrogen from wastewater. *Bioresour Technol*. **100**: 2910–2917.

Wu Y W, Li Q, Jin R, Chen W, Liu X L, Kong F L, Ke Y P, Shi H C, Yuan J C. 2019. Effect of low-nitrogen stress on photosynthesis and chlorophyll fluorescence characteristics of maize cultivars with different low-nitrogen tolerances. *J Integr Agric*. **18**: 1246–1256.

Yang F, Zhang S S, Cheng K, Antonietti M. 2019. A hydrothermal process to turn waste biomass into artificial fulvic and humic acids for soil remediation. *Sci Total Environ*. **686**: 1140–1151.

Yang F, Zhang S S, Fu Q, Antonietti M. 2020. Conjugation of artificial humic acids with inorganic soil matter to restore land for improved conservation of water and nutrients. *Land Degrad Dev*. **31**: 884–893.

Young A J. 1991. The photoprotective role of carotenoids in higher plants. *Physiol Plant*. **83**: 702–708.

Zeng L Z, Wang Y Q, Zhou J. 2016. Spectral analysis on origination of the bands at 437 nm and 475.5 nm of chlorophyll fluorescence excitation spectrum in *Arabidopsis* chloroplasts. *Luminescence*. **31**: 769–774.

Zhang X. 2021. Effects of fulvic acid on rice growth and nitrogen uptake under different nitrogen levels. *J Plant Nutr*. **48**: 1–14.

Zhang Z W, Wang Z Q, Wang Y, Lin T B. 2013. Effect of upper root-zone water stress on growth and development of maize roots and above-ground part. *J Henan Agric Sci* (in Chinese). **42**: 29–32.

Zhao Y, Hao Y, Cheng K, Wang L L, Dong W C, Liu Z Q, Yang F. 2024. Artificial humic acid mediated migration of phosphorus in soil: Experiment and modelling. *CATENA*. **238**: 107896.

Zhu X Y, Liang M, Ma Y. 2020. A review report on the experiments for the determination of root activity by TTC method. *Guangdong Chem Ind* (in Chinese). **47**: 211–212.